

Course 12.812, General Circulation of the Earth's Atmosphere
 Prof. Peter Stone
Section 5: Heat Budget

Observed Temperature Field

Temperature is the primary climate variable, and it is determined to a considerable extent by the heat budget. Thus we will look at a number of features of the T field that we would like to be able to explain and model. Figures 7.5, 7.6b, and 7.7 in Peixoto and Oort (1992) illustrate a number of properties of the T field.

I. Seasonal changes near the surface are:

- i) small near the equator ($\leq 1\text{C}$)
- ii) largest near the poles ($\sim 25\text{C}$)

II. Lapse rates, $\Gamma = -\frac{dT}{dz}$:

- i) typically $\Gamma \sim 5$ to 6 C/km in the lower troposphere \Rightarrow a statically stable

atmosphere with $\frac{\partial\theta}{\partial z} \sim 5 \text{ K/km}$, ($\theta =$ potential temperature) and thus a static

stability $\sim \Gamma_d - \Gamma \sim 5^\circ/\text{km}$ ($\Gamma_d = \frac{g}{c_p} = 9.8 \text{ K/km}$).

- ii) The atmosphere is conditionally unstable, as shown by $\partial\theta_E / \partial z$, where θ_E is the equivalent potential temperature of a saturated parcel,

$\theta_E = \theta \exp\{Lq_s / c_p T\}$, $\partial\theta_E / \partial z < 0 \Rightarrow \Gamma > \Gamma_{\text{moist adiabat}}$, particularly in the tropics.

III. Meridional gradients

- i) are larger in winter than summer, as shown by the temperature contrasts, $\Delta T = T_{\text{eq}} - T_{\text{pole}}$ at 500 mb, given in the table.

	Northern Hemisphere	Southern Hemisphere
winter	35°	40°
summer	15°	30°

- ii) have a stronger seasonal cycle in Northern Hemisphere

iii) are reversed in the stratosphere

IV. Longitudinal T contrasts are much smaller $\leq 6\text{K}$, and are strongly correlated with the continents, which are colder than the oceans in winter, warmer in summer.

Equations and Definitions

For an ideal gas, the equation for conservation of heat is

$$C_v dT + p d\alpha = \dot{H} dt$$

Where C_v = specific heat at constant volume, T = temperature, p = pressure, α = specific volume ($= \frac{1}{\rho}$ where ρ = density), \dot{H} = rate at which heat is added per unit mass of air by sources and sinks. In words, the heat added in time dt equals the change in the internal energy plus the work done by the unit mass of air on its surroundings. For a perfect gas,

$$p\alpha = RT \quad \text{and} \quad C_p = C_v + R$$

where R = gas constant, C_p = specific heat at constant pressure. Thus we may rewrite our energy equation in the form

$$C_v dT + p d\alpha = C_v dT + p \left(\frac{RdT}{p} - \frac{RT}{p^2} dp \right) = C_p dT - \alpha dp$$

$$\therefore C_p \frac{dT}{dt} - \frac{1}{\rho} \frac{dp}{dt} = \dot{H}$$

(N.B., since $\omega = \frac{dp}{dt}$, in pressure coordinates this is

$$\frac{\partial T}{\partial t} + u \frac{\partial T}{\partial x} + v \frac{\partial T}{\partial y} + \omega \left(\frac{\partial T}{\partial p} - \frac{RT}{C_p p} \right) = \frac{\dot{H}}{C_p}, \text{ and}$$

$$\frac{\partial T}{\partial p} = -\frac{1}{\rho g} \frac{\partial T}{\partial z} ; \quad \therefore \left(\frac{\partial T}{\partial p} - \frac{RT}{C_p p} \right) = -\frac{1}{\rho g} \left(\frac{\partial T}{\partial z} + \frac{g}{C_p} \right)$$

The equation of motion is

$$\frac{d\vec{v}}{dt} = -2\vec{\Omega} \times \vec{v} - \frac{1}{\rho} \nabla p - g\hat{k} + \vec{F} \text{ (friction) .}$$

We derive a kinetic energy equation by taking $\vec{v} \cdot$ equation:

$$\frac{d}{dt} \left(\frac{1}{2} v^2 \right) = -\frac{1}{\rho} \vec{v} \cdot \nabla p - wg + \vec{v} \cdot \vec{F}$$

$$\therefore \frac{dp}{dt} = \frac{\partial p}{\partial t} + \vec{v} \cdot \nabla p = \frac{\partial p}{\partial t} - \rho \frac{d}{dt} \left(\frac{1}{2} v^2 \right) - \rho wg + \rho \vec{v} \cdot \vec{F}$$

$$= \frac{\partial p}{\partial t} - \rho \frac{d}{dt} \left(\frac{1}{2} v^2 + gz \right) + \rho \vec{v} \cdot \vec{F}, \quad \text{since } w = \frac{dz}{dt}.$$

∴ Our energy equation becomes

$$C_p \frac{dT}{dt} - \frac{1}{\rho} \frac{\partial p}{\partial t} + \frac{d}{dt} \left(\frac{1}{2} v^2 + gz \right) = \dot{H} + \vec{v} \cdot \vec{F}$$

$$\therefore \rho \frac{d}{dt} \left(C_p T + gz + \frac{1}{2} v^2 \right) - \frac{\partial p}{\partial t} = \rho \dot{H}$$

From continuity, $\rho \frac{d}{dt}(\psi) = \rho \frac{\partial \psi}{\partial t} + \rho \vec{v} \cdot \nabla \psi$

$$= \frac{\partial}{\partial t}(\rho \psi) - \cancel{\psi \frac{\partial \rho}{\partial t}} + \nabla \cdot \rho \psi \vec{v} - \cancel{\psi \nabla \cdot \rho \vec{v}}$$

Also, $p = R\rho T$

$$\therefore \frac{\partial}{\partial t} \rho \left(C_p T + gz + \frac{1}{2} v^2 \right) - \frac{\partial}{\partial t} (R\rho T) + \nabla \cdot \rho \vec{v} \left(C_p T + gz + \frac{1}{2} v^2 \right) = \rho \dot{H} + \rho \vec{v} \cdot \vec{F}$$

and $\rho T(C_p - R) = C_v \rho T$;

$$\therefore \boxed{\frac{\partial}{\partial t} \rho \left(C_v T + gz + \frac{1}{2} v^2 \right) + \nabla \cdot \rho \vec{v} \left(C_p T + gz + \frac{1}{2} v^2 \right) = \rho (\dot{H} + \vec{v} \cdot \vec{F})}$$

$C_v T \equiv$ internal energy

$gz \equiv$ potential energy

$C_p T \equiv$ sensible heat or enthalpy

Generally we can neglect the kinetic energy. Oort (1971) calculated the total amount of energy in the Northern Hemisphere averaged over one year below 75mb. The result is

$$IE : 1.02 \times 10^{23} \text{ cal}$$

$$SH : 1.42 \times 10^{23} \text{ cal}$$

$$PE : 0.35 \times 10^{23} \text{ cal}$$

$$KE : 0.0007 \times 10^{23} \text{ cal}$$

Thus we will generally neglect $\frac{1}{2} v^2$.

$$\therefore \frac{\partial}{\partial t} \rho (C_v T + gz) + \nabla \cdot \rho \vec{v} (C_p T + gz) = \rho (\dot{H} + \vec{v} \cdot \vec{F})$$

In addition to radiative heating and changes of phase, $\rho \dot{H}$ also has contributions from molecular processes:

$$\rho \dot{H}_{\text{molec}} = \rho C_v K \nabla^2 T - \vec{v} \cdot \vec{F}$$

The last term represents the viscous dissipation of kinetic energy, and just cancels the $\vec{v} \cdot \vec{F}$ term introduced when we substituted from the kinetic energy equation. The first term represents the diffusion of heat, where K is the molecular conductivity for air, $K=0.18 \text{cm}^2/\text{sec}$.

Let us compare the magnitude of the diffusion term to a meridional transport term:

$$\frac{\rho C_v K \nabla^2 T}{\frac{\partial}{\partial y} (\rho v C_p T)} \sim \frac{\rho C_v K T / H^2}{\rho C_p v \Delta T / L} \sim \frac{KL}{vH^2}$$

If we take $H \sim$ scale height $\sim 10^6 \text{cm}$, $L \sim 10^3 \text{km} \sim 10^8 \text{cm}$, $K \sim 0.2$, $V \sim 10^3 \text{cm}/\text{sec}$, then the ratio is $0.2 \times 10^{-7} \ll 1$. Thus we can generally neglect the diffusion term. (Note that there is a similar molecular diffusion term in the moisture conservation equation which we have neglected. The justification is the same.)

Note however that the diffusion terms have the highest order vertical derivatives in the equation, and \therefore cannot be neglected if we want to include the molecular fluxes of $C_p T$ and $L_v q$ from the boundaries. In effect there are thin boundary layers near the boundaries where molecular processes cannot be neglected.

The contribution to \dot{H} by condensation and evaporation can be expressed in terms of q from the moisture conservation equation:

$$\rho \dot{H}_{\text{cond, evap}} = L_v C = -L_v \rho \frac{dq}{dt}$$

where $L_v =$ latent heat of condensation. Because of continuity, we can write

$$\rho L_v \frac{dq}{dt} = \frac{\partial}{\partial t} (\rho L_v q) + \nabla \cdot (\rho L_v \vec{v} q) = -L_v C$$

(Note that we are neglecting the latent heat released when water freezes. Freezing only occurs in the upper atmosphere where q is $\sim 10\%$ of surface values, and the enhancement

of L_v is only ~15%. Thus neglecting freezing only introduces errors $\lesssim 2\%$ into budget studies.)

Now substituting for the condensation contribution to \dot{H} in the heat equation we find that in effect we have added a new form of energy to our conservation equation, $L_v q = \underline{\text{latent heat}} = LH$. Now we have

$$\frac{\partial}{\partial t} \rho (C_v T + gz + L_v q) = \rho \dot{H} - \nabla \cdot \rho \vec{v} (C_p T + gz + L_v q)$$

For comparison with the other forms of energy, we note that in the Northern Hemisphere, $LH = 0.039 \times 10^{23}$ cal (Oort, 1971).

Now $\rho \dot{H}$ stands only for the radiative heating, the sole external drive for the atmosphere-ocean system. In equilibrium, the above equation states that radiative heating must be balanced at any point in the atmosphere by a divergence of dynamical fluxes of sensible heat, potential energy, or latent heat.

The radiative heating per unit volume, $\rho \dot{H}$, can also be expressed as the divergence of the radiative energy flux per unit area, \vec{F}_{rad} ,

$\rho \dot{H} = -\nabla \cdot \vec{F}_{\text{rad}}$; only the vertical divergence is significant, because of the small aspect ratio of the atmosphere:

$$\frac{\partial F_y / \partial y}{\partial F_z / \partial z} \sim \frac{F_y h}{F_z L} \sim \frac{h}{L} \sim 10^{-3} \ll 1, \text{ where } F_y \text{ and } F_z \text{ are typical horizontal and vertical long}$$

wave or short wave fluxes, and are comparable, and h is the scale height of the atmosphere. \therefore to a good approximation, we may write

$$\rho \dot{H} = -\frac{\partial F}{\partial z} \quad \text{where } F \text{ is the net vertical radiative flux.}$$

The horizontal divergence can be important when inhomogeneous cloud layers are present, but this effect is negligible when one looks at time averages over periods more than a few days (as we will be doing).

Boundary Conditions

To consider the overall atmospheric heat balance alone, we must add boundary conditions to the heat equation – i.e.: we must specify the radiative flux at the top of the

atmosphere (there are no dynamical fluxes at the top since $\rho w \rightarrow 0$) and all the radiative and dynamical fluxes at the bottom.

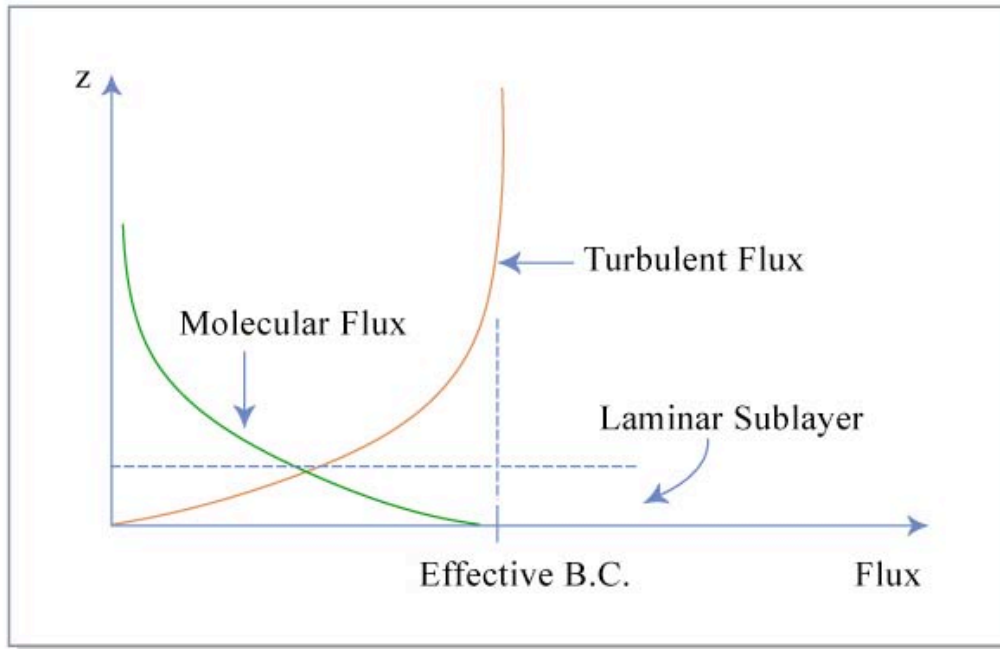


Figure by MIT OCW.

One might think that the dynamical flux should $\rightarrow 0$ at $z \rightarrow 0$ because of the frictional boundary condition $\bar{v} \rightarrow 0$ at $z = 0$. Formally, this is true. What actually happens is that the molecular fluxes which we have neglected in our equation cannot be neglected very near the ground. These molecular fluxes are taken up by the turbulent fluxes outside the surface layer, which is generally \leq a few meters. Since this depth is negligible compared to that of the troposphere, it is customary to apply the boundary condition for the molecular fluxes of sensible heat, water vapor, etc. directly to the dynamical fluxes. The radiative fluxes must also be specified at the ground.

In general, we will be interested in the climate system, i.e.: the atmosphere-ocean system of the earth as a whole, rather than the atmosphere in isolation. Then the lower boundary is specified to be deep enough that there are essentially no fluxes at it. For this whole system we have to add heat equations for the solid earth and oceans. The solid earth is incompressible, immobile, and impenetrable (as far as radiation is concerned). \therefore its balance is simply expressed by the equation

$$\frac{d}{dt}(\rho C_v T) = \mu \nabla^2 T + G$$

where

μ = molecular conductivity, and G represents heat gains or losses due to flows of groundwater.

Because of the small aspect ratio of the surface layer of the land in which appreciable T changes occur, this equation can be approximated by

$$\frac{\partial}{\partial t}(\rho C_v T) = \mu \frac{\partial^2 T}{\partial z^2} + G$$

C_v is in general a function of ground moisture.

The oceans are a nearly incompressible fluid and a single phase (except for sea ice forming at the surface, which must be dealt with separately), but they do contain currents and radiation can penetrate the surface layers. Molecular terms are again generally negligible compared to these terms. Thus the heat conservation equation for the oceans is

$$\rho C_v \frac{\partial T}{\partial t} + \nabla \cdot \rho C_v \vec{v} T = -\frac{\partial F}{\partial z}$$

For this multi-component system, we have to add as boundary conditions continuity of all the fluxes at the interfaces. If changes of phases occur at the interface (melting of snow, formation of sea ice, etc.), then we have to add sources or sinks of heat at the interface, or have separate equations for the heat balances of the sea-ice, etc. In this course we do not have to deal with the interfaces and the adjacent thin boundary layers.

Heat Budget Equation for Latitudinal Belts

For the annual mean heat budget, or seasonal extremes, we can neglect storage, \therefore our equation for the heat balance can be written concisely as

$$\nabla \cdot \overline{\rho \vec{v} \psi} = -\frac{\partial \bar{F}}{\partial z}$$

We can consider this as a generalized equation for all the different parts of the system – i.e. $\vec{v} = 0$ in the solid earth, $\psi = C_p T + \phi + L_v q$ in the atmosphere, $\psi = C_v T$ in the oceans, $F = F_{\text{rad}}$ in the atmosphere or ocean, $F = F_{\text{diff}}$ in solid earth. Now if we average over all z, it is convenient to use pressure coordinates for the left hand side:

$$\begin{aligned} \overline{\nabla \cdot \rho \bar{v} \psi} &= \overline{\rho \bar{v} \cdot \nabla \psi} = \rho \left(u \frac{\partial \psi}{\partial x} + v \frac{\partial \psi}{\partial y} + \omega \frac{\partial \psi}{\partial p} \right) \\ &= \rho \left\{ \frac{\partial (u\psi)}{\partial x} + \frac{\partial (v\psi)}{\partial y} + \frac{\partial (\omega\psi)}{\partial p} \right\}; \\ \therefore \int_{-\infty}^{\infty} dz \left(\overline{\nabla \cdot \rho \bar{v} \psi} \right) &= \frac{1}{g} \int_0^{p_0(-\infty)} \left\{ \frac{\partial}{\partial x} (\overline{u\psi}) + \frac{\partial}{\partial y} (\overline{v\psi}) + \frac{\partial}{\partial p} (\overline{\omega\psi}) \right\} dp \\ &= \frac{1}{g} \int_0^{p_0} \left\{ \frac{\partial}{\partial x} (\overline{u\psi}) + \frac{\partial}{\partial y} (\overline{v\psi}) \right\} dp \end{aligned}$$

because of the boundary condition $\omega \rightarrow 0$ at $p = 0$, and because we pick p_0 to be a large enough pressure (below the deepest oceans) that vertical flux is negligible at $p = p_0$. (We neglect the flux from the interior of the earth which is ~one thousandth of typical radiative fluxes at $p = 0$.) The right-hand side reduces to

$$-\int_{-\infty}^{\infty} \frac{\partial \bar{F}}{\partial z} dz = -\bar{F}(\infty), \text{ since } F \rightarrow 0 \text{ as } z \rightarrow -\infty, \text{ and of course at the top of the atmosphere}$$

$$F = F_{\text{rad}}.$$

$$\therefore \frac{1}{g} \int_0^{p_0(-\infty)} \left\{ \frac{\partial}{\partial x} (\overline{u\psi}) + \frac{\partial}{\partial y} (\overline{v\psi}) \right\} dp = -\bar{F}(\infty)$$

\therefore the net radiative heating at the top of the atmosphere is balanced by the divergence of fluxes of SH, LH, and PE in the atmosphere, and of SH in the oceans.

If we now integrate over all x , we obtain our budget equation for each latitude belt,

$$\frac{1}{g} \int_0^{p_0(-\infty)} \frac{\partial}{\partial y} [\overline{v\psi}] dp = -[\bar{F}(\infty)].$$

Each of these fluxes can be broken up statistically as

before:

$$[\overline{v\psi}] = [\bar{v} \bar{\psi}] + [\overline{v'\psi'}] + [\bar{v}^* \bar{\psi}^*] = (\text{MMC} + \text{TE} + \text{SE}) \text{ components.}$$

Since $\psi = C_p T + \phi + L_v q$, we are now concerned with not only the T and q fields in the atmosphere, which we have already looked at, but also the ϕ field. However, this is trivially related to the T field by H.E.:

$$\frac{\partial \phi}{\partial p} = -\frac{1}{\rho} = -\frac{RT}{p} \Rightarrow \phi(p) \text{ if } T(p) \text{ is given.}$$

Radiation Budget

In analyzing the heat balance of the atmosphere-ocean system as described by our budget equation above, our first step will be to consider just the radiation term in the equation. This is the term that drives the whole atmosphere-ocean system. Without external heating from the sun, communicated by radiation, there would be no motions in the atmosphere-ocean system (neglecting the small heat flux from the interior). Let us consider the overall radiation budget at any location on the planet by integrating through the atmosphere-ocean system:

$$\int_{-\infty}^{\infty} \rho H dz = - \int_{-\infty}^{\infty} \frac{\partial F}{\partial z} dz = -F(\infty) + F(-\infty)$$

Now define $R = -F(\infty)$ = net radiative flux into the atmosphere-ocean column. This is equal to the difference between the solar radiation absorbed, and the planetary radiation emitted, i.e.:

$R = Q(1 - \alpha) - I$	(units = energy/area/sec)
-------------------------	---------------------------

where Q = flux of solar radiation incident at the top of the atmosphere; α = planetary albedo = fraction of solar radiation reflected or scattered back into space without being absorbed; and I = amount of thermal radiation emitted to space by the ocean-atmosphere system. This division into solar and terrestrial radiation is very convenient because the wave-lengths of the two types of radiation are quite distinct, with very little overlap. (See Fig. 6.2a in Peixoto and Oort (1992)). This happens because the temperatures of the emitting sources are so different (Wien's Law). The surface of the sun is at ~6000K, while the surface of the earth is at ~300K. Thus solar radiation has a maximum in the short visual wave-lengths at ~.6 microns, while terrestrial radiation has a maximum in the long infra-red wavelengths at ~15 microns. Consequently, different observational and theoretical techniques are needed to analyze the two types of radiation.

The various terms in the radiation budget have substantial variations on a day to day basis (e.g. Q is a maximum during the day, $Q = 0$ at night), but we will consider their averages over many days.

We will consider the different components of R individually.

Incident solar radiation:

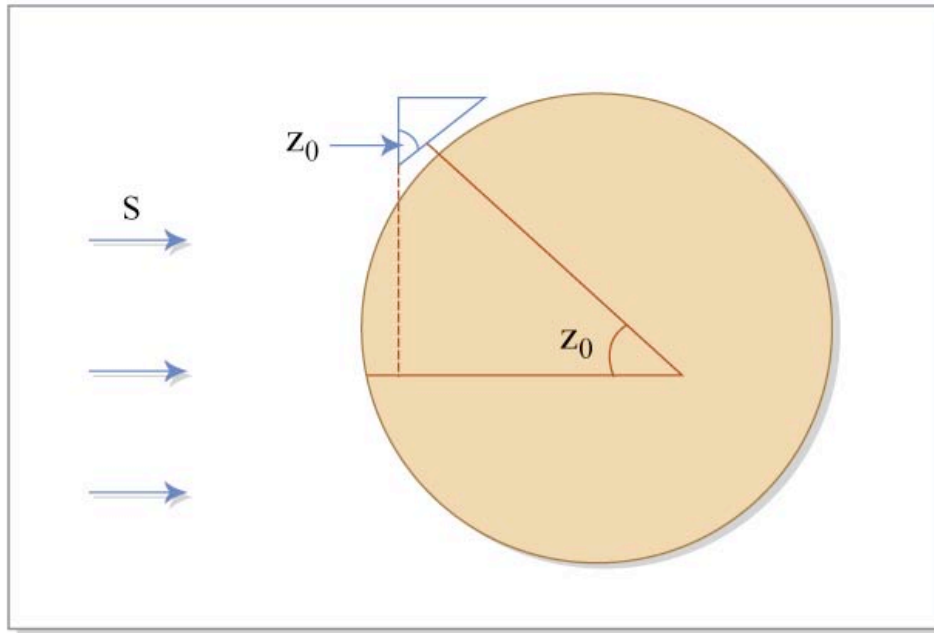


Figure by MIT OCW.

Let S = solar constant = annual mean amount of solar radiation incident on a unit area \perp to the direction to the sun at the position of the earth. Then the solar radiation incident on a unit area parallel to the surface of the earth at the top of the atmosphere, Q , is given by:

$$Q = \frac{S}{l^2} \cos(z_0)$$

Where l = distance of the earth from the sun, r , normalized by r_0 , $r_0^2 = \left(\frac{1}{\overline{r^2}} \right)$, (“ \bar{x} ”

indicates an annual average, thus $\left(\frac{1}{\overline{l^2}} \right) = 1$), and z_0 = solar zenith angle, the angle

between the directions to the sun and the zenith. z_0 depends on the latitude, ϕ , the time of day, measured by the hour angle, ω , and the season, measured by the solar declination, or solar latitude, δ_0 . ω is the angular distance between the meridian plane containing the sun and the meridian plane containing the zenith. From spherical geometry, the relation is

$$\cos z_0 = \sin \phi \sin \delta_0 + \cos \phi \cos \delta_0 \cos \omega.$$

For example, at the equinox, $\delta_0 = 0, \cos z_0 = \cos \phi \cos \omega$, and if we average over one day, then the mean of $\cos z_0$ is

$$\begin{aligned} \overline{\cos z_0} &= \frac{\int_{\text{day}} \cos \phi \cos \omega \, d\omega}{\int_{\text{day+night}} d\omega} = \frac{\int_{-\pi/2}^{\pi/2} \cos \phi \cos \omega \, d\omega}{\int_{-\pi}^{\pi} d\omega} \\ &= \frac{\cos \phi \sin \omega \Big|_{-\pi/2}^{\pi/2}}{2\pi} = \frac{\cos \phi}{\pi} = \overline{\cos z_0} \end{aligned}$$

In general, we are not concerned with diurnal effects, but with averages of $\cos z_0$ over 24 hours. At times of year other than the equinox, this becomes more complicated, because the length of the day varies. Let ω_0 = hour angle of sunset.

$$\begin{aligned} \therefore \overline{\cos z_0} &= \frac{\int_{-\omega_0}^{\omega_0} (\sin \phi \sin \delta_0 + \cos \phi \cos \delta_0 \cos \omega) \, d\omega}{\int_{-\pi}^{\pi} d\omega} \\ &= \frac{\omega_0 \sin \phi \sin \delta_0 + \cos \phi \cos \delta_0 \sin \omega_0}{\pi} \end{aligned}$$

and ω_0 is by definition the value of ω when $Q = 0$, i.e.: $\cos \omega_0 = -\tan(\phi) \tan(\delta_0)$. From this we can calculate $\overline{Q}^{\text{1day}}$ as a function of latitude and season.

The results for the two solstices are shown in the table on p.5 of Budyko, Climate and Life, 1974. It shows the latitudinal distribution of Q at the solstices in Kcal per cm^2 per day, assuming that $S_0 = 2 \text{ cal/cm}^2/\text{min}$. Note that $1 \text{ Kcal/cm}^2/\text{day} = 483 \text{ W/m}^2$.

From the table we see that:

- 1) The solar radiation is about 7% stronger in December than June, because the earth reaches perihelion early in January (over very long periods, this changes).
- 2) In general the intensity of the radiation increases from the winter pole to the summer pole, with maximum right at the summer pole, because of the increasing length of the day.
- 3) There are slight minima at 60° in the summer hemisphere, because the decrease in the sun's altitude temporarily more than compensates for the increased length of the day.
- 4) The latitudinal gradient in the summer hemisphere is much weaker than in the winter hemisphere, because the changes in the altitude of the sun and in the length of the day reinforce each other in the winter hemisphere, but tend to compensate

each other in the summer hemisphere. The annual average distribution of Q is given with 2% accuracy by the formula

$$Q = \frac{S_0}{4} (1 + S_2 P_2(x)) ;$$

$x = \sin(\phi)$; $P_2 = \frac{1}{2}(3x^2 - 1)$; $S_2 = -0.48$; the factor 4 comes from the area of the earth.

The total amount of energy intercepted by the earth is $S_0 \pi R^2$, but if we average over the surface area of the earth, $4\pi R^2$, the mean is $\frac{S_0}{4}$. Note that the differential heating between equator and pole is

$$Q(0) - Q(1) = \frac{S_0}{4} \left(-\frac{3}{2} S_2 \right) = \frac{3}{8} S_0 |S_2| = 250 \text{ W/m}^2 .$$

The actual value of the solar constant, S_0 , as determined by recent satellite measurements is $S_0 = 1366 \text{ W/m}^2 = 1.97 \text{ cal/cm}^2 / \text{min}$ (see Fig.1 from Eos, Trans. AGU, 84, No.22., 2003).

The major uncertainty is the natural variability. Fluctuations of a few tenths of a percent over periods of a few weeks are commonly observed, and they are inversely correlated with sunspots ($\Delta S \cong \frac{1}{4} \% \cong 3 \text{ W/m}^2$), because the regions surrounding sunspots are brighter than normal. Known fluctuations of sunspots in past centuries suggest that S_0 may have changed by a few .1%.

Albedo: Typical albedoes associated with various surfaces that reflect solar radiation are shown in the table.

Aerosols	Small but highly variable
Soil, rocks, vegetation	.1 to .3
Water	.02 to .2
Snow and ice	.6 to .8
Cb (clouds)	~.9
Cu (clouds)	~.7
St (clouds)	~.5
Ci (clouds)	~.2
Rayleigh Scattering	~.05

The values are highly variable. They depend not only on the composition of the surface, but also on the solar zenith angle and the roughness of the surface (e.g., surface water waves). Cloud albedoes depend on the nature (ice or water), depth of the cloud, and size

of the cloud particles, as well as solar zenith angle. Clouds account for ~1/2 of the global mean albedo. (Global cloud cover is ~50%.) Most of the rest is due to snow and ice, and small amounts are due to other surfaces and atmospheric molecules and aerosols (haze, etc.) Cumulus clouds are important because of large albedoes, stratus and cirrus because of large cloud covers.

Reasonably good measurements of mean albedoes and global albedoes (i.e.: time averages which include all of the above phenomena) are available from satellite observations. Stephens et al (1981)¹ used satellite observations from 48 months during 1964-1977. (Complete data was available from at least 3 years for each month so good monthly and annual averages could be obtained.) Their results for global and hemispheric values are given in the table.

Planetary Albedo
Units: percent

	DJF	MAM	JJA	SON	Annual	error
Northern Hemisphere	30	33	31	29	31	
Southern Hemisphere	31	28	27	30	30	
Global	31	30	30	30	30	± 1

Source: Stephens et al., 1981

(N.B. For measuring albedoes, the satellite observations have a potentially serious bias: they were all made from sun synchronous polar orbiters, with the subsatellite point in most cases being mean local noon. ∴ there was very limited coverage of times of day and phase angles. ∴ the necessary phase integrals could not be calculated directly from the observations. This is particularly serious for polar regions, where zenith angles are low.)

We note that the two hemispheres appear to have different seasonal effects. The Northern Hemisphere has the highest albedo in spring. This difference could be due to the different feedbacks associated with the two dominant contributors to the albedo: If solar heating is increased, as in summer, then one would expect convection and cloud cover to increase, and snow and ice cover to decrease. The former effect tends to increase the albedo, the latter to decrease it (i.e. a negative feedback vs. a positive feedback.) Perhaps the cloud changes dominate in the Southern Hemisphere, and the ice and snow effect is more important in the Northern Hemisphere. The ice and snow feedback is much more dependent on land surface. The hemispheres are asymmetric, with most land in the Northern Hemisphere and one would expect this to enhance both feedbacks in the Northern Hemisphere. In the Southern Hemisphere land is almost non-existent, so the cloud feedback dominates while in the Northern Hemisphere the ice and snow feedback is much stronger and is dominant. In any case the seasonal changes are small and may not be indicative of the feedbacks because equilibrium is never achieved for ice and snow.

¹ Ardanuy et al (1992, J. Climate, 5, 1126) have analyzed 4 years of Nimbus 7 data (Nimbus 7 was also in a sun synchronous orbit.) However their results are essentially no different from Stephens et al, and they give less information, e.g., no error estimates.

Stephens et al also computed the mean albedo as a function of latitude and found the results illustrated in the figure below. As one would expect, the polar regions have the greatest albedoes, with the Antarctic being brightest. The minimum occurs in the southern subtropics. They also computed maps showing longitudinal variations in $\bar{\alpha}$. The albedo is highly correlated with land surfaces, generally being higher over land. Typical longitudinal differences are $\Delta\bar{\alpha} \sim 0.10$.

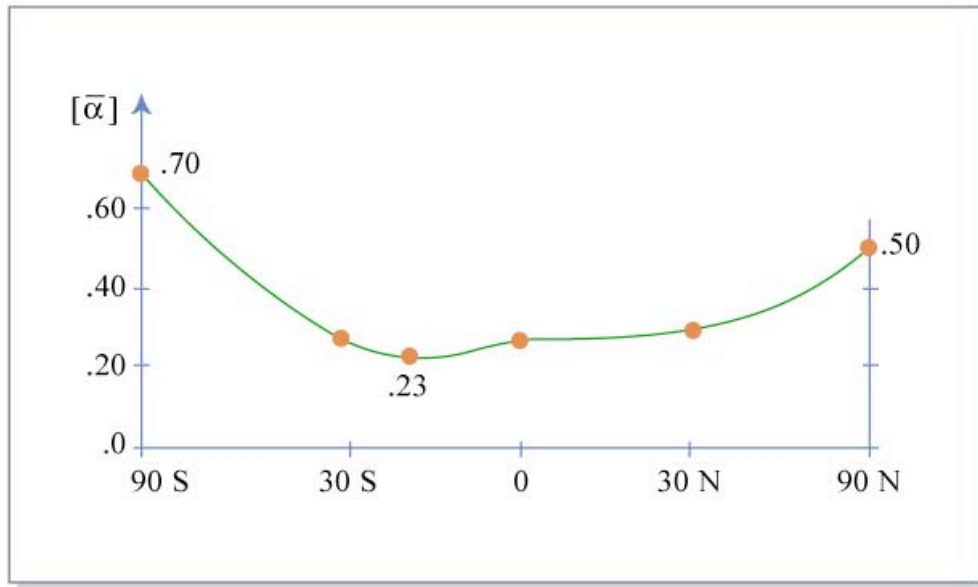


Figure by MIT OCW.

Short wave spectra show that $\sim 30\%$ of $Q(1 - \alpha)$ is absorbed in the atmosphere, $\sim 70\%$ at ground.

Planetary Radiation: The atmosphere is optically rather thick in the infra-red and \therefore relatively little of the planetary radiation emitted from the surface ($< 5\%$) escapes to space. (See fig. 6.2b in Peixoto and Oort (1992)). Most comes from higher up, in particular, thermal emission from clouds and water vapor. CO_2 and O_3 are also important emitters, particularly in the stratosphere, and some surface emissions escape in arid regions, where it is not blocked effectively by water vapor and clouds. The table from Stephens et al (1981) shows the global and hemispheric values of long wave emission.

Thermal Emissions

Units: $\frac{W}{m^2}$

	DJF	MAM	JJA	SON	Annual
Northern Hemisphere	222	237	242	230	233
Southern Hemisphere	238	237	232	232	235
Global	230	237	237	231	234±7

Source: Stephens et al., 1981

The effective temperature, T_e , is defined as the temperature of a black body which would emit the observed thermal radiative flux, i.e.

$$I = \sigma T_e^4$$

Thus if we put in the global mean thermal emission, $\bar{I} = 236 \pm 7 \frac{W}{m^2}$, we calculate

$T_e = 255^\circ \pm 2^\circ$. Since the observed mean surface temperature is 288K, this implies that the thermal emissions to space come on average from an elevation of about 6km. It also implies that the earth's surface is about 33K warmer than it would be if there were no greenhouse absorbers in the atmosphere. The satellite observations of global mean albedo, $\bar{\alpha} = 0.30 \pm 0.01$, imply that the global mean absorption of solar energy is

$\frac{S_o}{4}(1 - \bar{\alpha}) = 239 \pm 3 \frac{W}{m^2}$. Thus, within the error bars, the climate system is in global radiative equilibrium, i.e. the absorbed energy equals the emitted energy. The errors are however unfortunately large, too large to detect global warming. The total increase in the flux of heat into the system since the beginning of the industrial revolution due to

increases in greenhouse gases is estimated to be about $2 \frac{1}{2} \frac{W}{m^2}$, and because the system

has warmed up somewhat, and because there has been some cooling due to increases in aerosols, model estimates of the imbalance of energy at the top of the atmosphere are ~1

to $1 \frac{1}{2} \frac{W}{m^2}$.

The seasonal variations are surprisingly small ($\Delta T_e \sim 5^\circ$), given that $I \sim T_e^4$. This is because the effective radiating layers are higher up in warmer months, so that the effective radiating temperature does not change very much: As T increases, the water vapor content of the atmosphere increases, \therefore the total optical depth increases, so that the level of optical depth unity, which is the effective radiating layer, moves up. The small seasonal changes are in the direction one would expect.

The annual mean latitudinal distribution of \bar{I} is shown in Fig. 3a of Stephens et al (1981). The hemispheres are not completely symmetric. The dip near the equator is due to the ITCZ. Time mean longitudinal variations in mid and high latitudes are very small,

but in low latitudes they are noticeable. The lack of variations in mid and high latitudes is due to the transient nature of the large scale circulation systems, while the variations in low latitudes are due to the semi-permanent nature of the circulation systems (such as the monsoons), with consequent systematic longitudinal variations in cloud cover, etc. These low latitude longitudinal variations are typically $\sim 20 \text{ W/m}^2$.

Net absorption in the climate system:

From the above results, it is now possible to calculate the net amount of radiation absorbed in the climate system from the Budget Equation, $R = Q(1 - \alpha)$. The table from Stephens et al (1981) shows the global and hemispheric budgets (R averaged over latitude and longitude). (Stephens et al used $S_0 = 1376 \text{ W/m}^2$.)

Net Absorption
Units: W/m^2

	DJF	MAM	JJA	SON	Annual
Northern Hemisphere	-51	+31	+63	-20	+5
Southern Hemisphere	+84	-30	-67	+43	+7
Global	+16	0	-2	+11	+6 ± 7

Source: Stephens et al., 1981

We note that not only the global budget, but also the annual hemispheric budgets are in balance, within the accuracy of the measurements. However the expected seasonal effects are observed: net heating in summer and cooling in winter.

We can see the latitudinal variation of $[R]$ from Fig. 6 in Vonder Haar and Suomi (1971). Stephens et al did not have an equivalent graph, but their results are very similar. The annual mean is shown in Fig. 3a of Stephens et al (1981).

The December/January/February and June/July/August curves are not symmetric about the equator; seasonal variations are larger at the North Pole than at the South Pole. Note the reversals near the winter poles. Here there is no solar radiation, and \therefore in $R = Q(1 - \alpha) - I$, the latitudinal change in I alone is present. Q decreases with latitude in the winter hemisphere, and so does I, and \therefore R increases near the winter poles. Elsewhere the Q variation dominates.

The net radiative heating, R, is the basic drive for the atmosphere-ocean system. The latitudinal variation in R gives rise to latitudinal temperature gradients \Rightarrow pressure gradients \Rightarrow motions. In the annual mean the differential heating must be balanced by dynamical fluxes of heat from low to high latitudes. The larger gradient of R in winter than in summer is consistent with the larger winter temperature gradients we noted

earlier, and the R gradient is of course ultimately traceable to the differential solar heating, $Q(\phi)$. The longitudinal gradients of R are quite weak, compared to the latitudinal gradients. They occur mainly in low latitudes, with typical contrasts $\sim 20 \text{ W/m}^2$ as compared to the latitudinal contrasts $\sim 100 \text{ W/m}^2$.

A more recent analysis of the net radiative heating of the globe, from Nimbus 7 measurements, is shown in Fig. 5 of Ardanuy et al (1992). There is again an average imbalance (net heating of the globe) of 6 W/m^2 . However Ardanuy et al's estimates of the errors are $+1.3 \text{ W/m}^2$ due to undersampling of the polar caps, $+1.6 \text{ W/m}^2$ due to an overestimate of the solar constant (why it is overestimated, they don't say), and $\pm 3 \text{ W/m}^2$ due to inaccurate calibration of the thermal radiation. Thus the imbalance may be all error, but is consistent with some global warming.

Effects of Clouds on Radiative Balance: Clouds have two effects: cooling (by reflecting SW radiation) and warming (by blocking LW emission to space). Their net effect is not so easy to determine, especially on a global basis. Low clouds tend to have a net cooling effect, while high clouds generally have a net warming effect. Only recently has good enough satellite data been gathered to allow one to calculate the net cloud effect.

The basic method is to separate out times and areas where clouds are absent (low α , high I) and use that data to compute a radiation budget without clouds. Then by comparing with the actual budget averaged in area and in time, a measure of the effect of the clouds can be calculated. This measure is called cloud forcing and is defined as

Cloud forcing = -average(clear + cloudy) flux value + average(clear) flux value = CF, i.e.

$$CF = \bar{R} - \bar{R}(\text{clear})$$

$$= (I + \alpha \bar{Q})_{\text{clear}} - (I + \alpha \bar{Q})_{\text{mean}} = CF_{\text{sw}} - CF_{\text{LW}}$$

$CF > 0 \Rightarrow$ clouds are heating the climate system.

The cloud forcing was calculated by Kyle et al (1991) using Nimbus 7 earth radiation budget data. Nimbus 7 was in a sun-synchronous orbit, so the data does not have good phase angle coverage. The results appear in a NASA report (Kyle et al., 1991, NASA reference publication 1263). The annual mean results (based on June 1979-May 1980) are shown in Fig. 2 of the report. They regard the results in polar regions as unreliable, because it is difficult to separate cloud albedo effects from snow/ice albedo effects. We see that the net effect is very small in low latitudes, but there is a significant cooling in mid-latitudes. The global mean value is ~ -15 to -20 W/m^2 .

Mean Annual Meridional Transports in the Atmosphere: As we saw above, the differential radiative heating must be balanced at least on an annual basis by meridional fluxes of sensible heat in the atmosphere and ocean and latent heat and potential energy

in the atmosphere. We first turn our attention to the atmospheric fluxes. We will discuss these using the results presented by Oort, 1971, and Oort & Peixoto (1983), who give more detail than later analyses. It is instructive to classify the atmosphere fluxes in terms of their transport mechanism – i.e., fluxes by the mean meridional circulations, the standing eddies, and the transient eddies. Then we will break down each kind of transport into the different energy components, i.e.: SH, LH, and PE. The Oort (1971) analysis is based on ~540 daily reporting rawinsonde stations over the Northern Hemisphere and tropics for the period May, 1958-April, 1963. The Oort & Peixoto analysis is global, for the period May, 1963-April, 1973, and also includes all available surface ship reports. In the latter global analysis there are ~1100 rawinsonde stations included. We use the Oort (1971) analysis for looking at the components of the MMC transports because Oort and Peixoto did not do this. Note that I have put the later analyses in terms of more conventional units, but not the Oort (1971) results since some detail would be lost. However I do include the total MMC transport from Oort & Peixoto (1983) in PW. I do not include the southern hemisphere because O&P themselves say that their results from 30S to 70S are only “tentative” because of poor station coverage, and the tropics are very uncertain because of the problems in determining a $[V]$ which conserves mass. The results are shown in the tables:

Annual mean Energy Transport by Mean Meridional Circulations

Units: 10^{19} cal/day (=0.48PW)

Latitude	10S	0	10N	20N	30N	40N	50N	60N	70N
SH	13	-1	-11	-5	1	2	2	0	-1
PE	-20	2	16	9	-1	-4	-4	0	2
LH	5	1	-4	-3	0	1	1	0	0
Total	-2	1	2	1	0	-1	-1	0	1

Source: Oort (1971)

Total	-1.0	.6	.8	.3	-.2	-.5	-.6	-.1	.2
-------	------	----	----	----	-----	-----	-----	-----	----

(units: Petawatts)

By Transient Eddies (PW)

Latitude	10S	0	10N	20N	30N	40N	50N	60N	70N
SH	0	0	-.2	0	.9	2.1	2.1	1.5	0.7
LH	-.5	0	.5	.8	1.1	1.1	.8	.5	.2
Total	-.4	0	.3	.6	1.9	3.3	2.8	1.9	.8

By Standing Eddies (PW)

Latitude	10S	0	10N	20N	30N	40N	50N	60N	70N
SH	-.1	0	0	.1	.1	.2	.7	.6	.1
LH	-.1	-.1	0	.4	.3	.1	.1	.1	0
Total	-.1	-.1	0	.4	.3	.2	.6	.6	.1

Source: Oort & Peixoto (1983)

For the MMC, the first table gives the annual mean transports of SH, PE, and LH, and the total transport in units of 10^{19} cal/day. Although the individual heat terms appear large, there is considerable cancellation and the net transport is considerably smaller. There is a net poleward heat transport in low latitudes, corresponding to the direct Hadley cell, and a net equatorward transport in mid latitudes, corresponding to the indirect Ferrel cell. There is a suggestion of a direct cell in high latitudes. These results are easily explained in terms of the observed annual mean meridional stream function described before. Since T decreases with height, so that the upper branches of the cells are relatively colder, we see that SH will on net be equatorward in low latitudes and poleward in mid-latitudes.

Recalling that the atmosphere in the mean is statically stable, i.e.

$$SH + PE = C_p T + gz = C_p (T + \Gamma z) = C_p \int_0^z \left(\frac{dT}{dz} + \Gamma \right) dz + C_p T_0$$

and $\frac{dT}{dz} + \Gamma > 0$, \Rightarrow SH + PE increases with height, thus the poleward branch dominates,

\therefore SH + PE yields a net poleward flux in low latitudes, and equatorward in mid latitudes.

LH is concentrated in regions of high temperature because of the Clausius-Clapyron relation, i.e., near the ground, and \therefore its direction of net transport is determined by the direction of the lower branch of each cell. Thus, the LH tends to compensate SH+PE, and the total is a small residual. In the tropics the eddy transports are small compared to the MMC transport, and thus we could expect its net transport to be thermodynamically direct, i.e., poleward, and it is.

Next we consider the annual mean transports by the transient eddies, tabulated above in PW. Here we have not bothered to tabulate the PE transport, because it is so small—at most 5% of SH or LH. (This is because the Rossby number is small).

These fluxes are primarily confined to mid and high latitudes. The transient eddy flux is considerably larger than the fluxes due to the mean circulation in most latitudes. The flux of LH peaks at lower latitude than the flux of SH, again because of the Clausius-Clapyron relation, which forces most of the water vapor to be concentrated in warmer, low latitudes.

Next we consider the annual mean transports by the standing eddies, tabulated above in PW. Again, PE transports are negligible.

The net flux is as small as that due to the mean meridional motions. They occur at mid and high latitudes since this is where most of the topography which drives standing eddies is located. Again, LH peaks south of SH.

Now we can add up all these components to get F_A , the total atmospheric transport. Peixoto and Oort's (1983) result is shown in Fig. 4b of Carissimo et al (1985). They estimated the error from looking at the inter-annual variations, and concluded that the error was $\pm 5\%$. However, this does not allow for the sparseness of the rawinsonde network.

Other analyses using modern data assimilation techniques, e.g. Trenberth and Caron (2001), who used the ECMWF and NCEP re-analyses get a much stronger result (see their Fig. 2). Trenberth & Caron only calculated the total transport, and to do so they had to balance the data. They use a variational method to minimize the correction to the three-dimensional velocity field, subject to the constraint $\nabla \cdot \vec{v} = 0$, using $z = H \ln \frac{P_{00}}{p}$ as the vertical coordinate (see Trenberth et al., 1995, *J. Climate*, 8, 692). Trenberth and Caron noted that the correction is small for ECMWF but large for NCEP.

In the Northern Hemisphere, where the data is best, Peixoto & Oort have a peak transport of 3.0PW, while Trenberth and Caron find 4.6 for ECMWF, 5.2 for NCEP. However, both analyses have systematic errors. Peixoto and Oort's method smooths the fields in data sparse areas like the oceans, and \therefore tends to miss out eddies and underestimate their transports. As we discussed earlier, Oort (1978) tested his technique by applying it to GCM data. The result is shown in Fig. 14 of Oort (1978). We can estimate the systematic error in the annual mean by averaging the results for January and July. We

find that the model transport at 40N is 25% larger than given by Peixoto and Oort's technique, $\Rightarrow F_A(\text{peak}) \cong 3.75\text{PW}$.

However, the ECMWF/NCEP models may also have a bias. As shown in Fig. 2b of Gleckler et al (1995), an earlier version of the ECMWF model gave more transport by itself than the analysis result. Thus the ECMWF data assimilation may be overestimating the transport in data sparse areas. The earlier analysis by Trenberth and Solomon (1994), shown in Fig. 2b of Gleckler et al (1995), gave a Northern Hemisphere peak of 3.9PW. The earlier version of ECMWF's model by itself gave a peak of 4.4. The increase to 4.6 in Trenberth and Caron (2001) is probably because the model and its resolution have changed. A reasonable compromise estimate is that $F_A(\text{peak in Northern Hemisphere}) = 4 \pm 1\text{PW}$.

We will revisit this after considering the next topic.

Oceanic Heat Transport: This is all in the form of internal energy ($C_v T$). There are very few direct measurements of this flux, because of the lack of an ocean observing network – only a few dedicated observing programs at given locations have yielded sufficient v and T data to calculate this (e.g., Bryden et al, 1991). Rather, we will look at results from two indirect ways of calculating it. One calculates it as a residual from atmospheric data (Vonder Haar & Oort, 1973, JPO, 3, 169; Carissimo et al., 1985; Jiang et al., 1999; Trenberth and Caron (2001)). The other uses an ocean model run in a data assimilation mode, although in this case it is in effect an equilibrium simulation, constrained by observational results like those of Bryden et al (1991). The most recent of this second type of analysis are those of Macdonald and Wunsch (1996) and Ganachaud and Wunsch (2002).

The first technique uses our time mean balance equation:

$$\frac{1}{g} \int_0^{P_a} (\nabla_H \cdot \overline{\vec{v}\psi}) dp = \bar{R} = \frac{1}{g} \nabla_H \int_0^{P_a} (\overline{\vec{v}\psi}) dp.$$

$$\text{Let } \vec{f}_a = \int_0^{\infty} \rho \overline{\vec{v}\psi} dz = \frac{1}{g} \int_0^{P_a} \overline{\vec{v}\psi} dp = \text{atmospheric transport,}$$

$$\text{and } \vec{f}_o = \frac{1}{g} \int_{P_s}^{P_a} \overline{\vec{v}\psi} dp = \text{oceanic transport.}$$

$$\therefore \nabla_H \cdot (\vec{f}_a + \vec{f}_o) = \bar{R}$$

$$\text{or } \nabla_H \cdot \vec{f}_o = \bar{R} - \nabla_H \cdot \vec{f}_a = -\bar{F}_s, \text{ where } F_s = \text{net surface heat flux.}$$

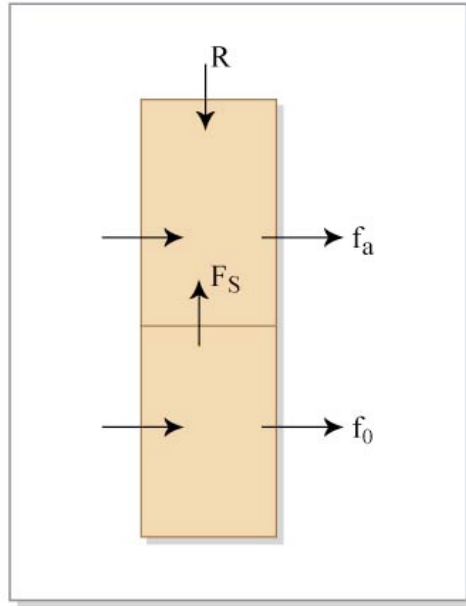


Figure by MIT OCW.

Now integrate around a latitude belt and define

$$F_0 = \frac{a \cos \phi}{g} \int_0^{2\pi} d\lambda \int_{P_s}^P \overline{v\psi} dP$$

$$= \frac{2\pi a \cos \phi}{g} \int_{P_s}^P \left[\overline{v\psi} \right] dP$$

= total meridional flux of heat across a latitude ϕ in the ocean. Similarly for the atmosphere

$$F_A = \frac{2\pi a \cos \phi}{g} \int_{P_s}^P \left[\overline{v\psi} \right] dp,$$

$$\therefore \frac{1}{2\pi a^2 \cos \phi} \frac{\partial F_0}{\partial \phi} = \left[\overline{R} \right] - \frac{1}{2\pi a^2 \cos \phi} \frac{\partial F_A}{\partial \phi} = \left[\overline{F_s} \right]$$

Vonder Haar and Oort and Carissimo et al inserted the observations of \overline{R} and \overline{F}_A into this equation and integrated to find \overline{F}_0 . Note however, that because of errors in the analysis, the surface fluxes over land implied by \overline{R} and \overline{F}_A will not necessarily be zero, although they should be in equilibrium. However, Jiang et al and Trenberth and Caron excluded these errors from their calculation of \overline{F}_0 by setting $\overline{F}_s = 0$ over land. This is clearly

better. Note that one can also calculate \bar{F}_0 for different ocean basins by just averaging \bar{F}_s over the appropriate longitudes.

One problem remains in calculating F_0 : because of errors in the data, we do not get global

equilibrium, i.e.: $\int_{-\pi/2}^{\pi/2} 2\pi a^2 \cos\phi [\bar{R}] d\phi \neq 0$, and $\int_{\text{ocean}} \bar{F}_s dA \neq 0$. Thus, unless one balances

the data, you do not get $F_0 = 0$ at both poles. Carissimo et al tried various techniques for modifying $[\bar{R}]$ – they all give very similar results and one could just as well use the

simplest, i.e., subtract a constant flux/area from \bar{R} . Jiang et al. and Trenberth and Caron instead just balanced \bar{F}_s over the oceans, $\int_{\text{ocean}} \bar{F}_s dA = 0$. To do this, Trenberth and Caron

assumed that all of the error in F_s is in the Southern Hemisphere, and they modified the Southern Hemisphere values of F_s by introducing a correction which increased linearly from zero at 30S to Antarctica. Jiang et al assumed a uniform error in F_s over all the oceans.

Jiang et al.'s results are in better agreement with the results from the data assimilation technique. Their results are shown in Fig. 3b of their 1999 paper. (Also shown are the individual transports for the two ocean basins – note equatorward transport in the South Atlantic.) They are compared with the MacDonald and Wunsch results. Note that at 45N (peak in \bar{F}_A) Carissimo et al had $F_0 \sim 1PW$, Jiang et al and MacDonald and Wunsch $\sim 1/2PW$.

The important results may be summarized as follows:

- 1) $\bar{F}_0 \sim \bar{F}_A$ in magnitude ($\bar{F}_0 \sim 2PW$ in Northern Hemisphere, $\sim 1PW$ in Southern Hemisphere; $F_A \sim 4PW$ in both);
- 2) \bar{F}_0 peaks at low latitudes ($\sim 15^\circ$), \bar{F}_A peaks at $\sim 45^\circ$;
- 3) $\bar{F}_A + \bar{F}_0$ peaks at 35° in both hemispheres, and $\bar{F}_A \sim \bar{F}_0$ at 35° .

Thus we conclude that the oceans are of fundamental importance in establishing meridional temperature variations and climate. Note that $\bar{F}_0 > \bar{F}_A$ in low latitudes: at 15N, $\bar{F}_0 \sim 2PW$; $\bar{F}_A \sim 1PW$.

4) And finally, we note that the total dynamical transport, $\bar{F}_A + \bar{F}_0$, is to a very high accuracy anti-symmetric about the equator – e.g., see Fig. 2 in Trenberth and Caron (2001). This implies that hemispheric asymmetries in mountains, ocean area, etc., are not important in determining the total poleward flux. This is apparently because there is a lot of negative feedback between different components of the flux (Stone, 1978, Dyn. Atmos. Oceans, 2, 123).

Now let us consider the atmospheric heat transport again. We saw earlier that there are substantial differences between the station-based and re-analysis-based results. In general the investigators did not attempt any comprehensive analysis of the errors associated with their results. Recently Wunsch (2005, *J. Climate*, **18**, 4374) has attempted to do this, by reversing the residual calculation, i.e. by calculating \bar{F}_A from \bar{F}_0 and $[\bar{R}]$. Error estimates are available for the last two, and he simply propagated the error estimates, assuming that they are independent. The satellite (ERBE) data is out of balance by about 6W/m^2 averaged over the whole earth, which implies a transport $\sim 3\text{PW}$ at one pole. He assumed a random error of 5.5W/m^2 , based on the interannual variations. He also balanced the data by minimizing the rms deviations of the corrected observations from a prior distribution derived by Stone (1978), i.e.,

$$\bar{F}_A + \bar{F}_0 = \frac{\pi R^2}{4} S_0 S_2 (1 - \alpha_0) \sin \phi (\sin^2 \phi - 1),$$

where R is the radius of the earth, S_0 is the solar constant, S_2 is the previously defined 2nd coefficient in the Legendre polynomial expansion of \bar{Q} , and α_0 is the unweighted global mean of $[\bar{\alpha}]$. Taking $S_0 = 1366 \text{ W/m}^2$, $S_2 = -0.48$, and $\alpha_0 = 0.32$, we have $\bar{F}_A + \bar{F}_0 = 14\text{PW} \sin \phi (1 - \sin^2 \phi)$.

The ocean data and error estimates come from Ganachaud and Wunsch (2002). The ocean transports were only calculated at 6 latitudes, where the data is best. Values at other latitudes were interpolated linearly.

The results are shown in Fig. 3 (right hand side) of Wunsch (2005). The error bands correspond to \pm one standard deviation. The resulting ranges for the peak values of \bar{F}_A are: Northern Hemisphere: 3.0 to 5.2PW; and Southern Hemisphere: -4.0 to -6.7PW, consistent with all the earlier results.

Seasonal Changes in Atmospheric Transports

(N.B. Oort & Peixoto (1983) do not give enough data to examine the seasonal changes adequately. Thus we follow Oort (1971) and use his units ($10^{19}\text{cal/day} = .48\text{PW}$).

First we look at the seasonal change in the flux by the mean meridional circulations. The division between SH, LH, and PE is proportionately the same as in the annual means, with the sum being small compared to the individual terms, so we will only look at the net transport, SH + LH + PE, in 10^{19}cal/day . January and July are the extreme months.

Latitude	-10	0	+10	+20	30	+40	+50	+60	+70
January	1	3	4	3	-2	-3	-2	1	1
July	-6	-2	1	0	-1	0	-1	0	1

We see here a substantial seasonal change in equatorial regions, where the flux changes sign. This is due to the substantial seasonal changes in the Hadley cells. In general there are two Hadley cells, as indicated in our picture of the mean stream function, one in each hemisphere. These two cells move north and south seasonally with the sun, and the

summer cell is much weaker than the winter cell – i.e. the northern cell dominates in January, and the southern cell in July.

The direction of the mean flow near the equator in July has completely reversed, as the Southern Hemisphere Hadley cell has moved into the position of the Northern Hemisphere Hadley cell, and the latter has virtually disappeared. The mid-latitude Ferrel cell persists in both seasons, and is apparent in the net transport, but is much weaker in the summer. The direct polar cell is always weak. Note that the transports in January & July are generally much larger than the mean annual transport, since the changing position of the two Hadley cells almost negates their changing strengths. Oort calculated the annual transports by calculating $\left[\overline{\rho v}\right]\left[\bar{x}\right]$, two ways, first using a full year for his averaging period, and then using the individual twelve calendar months for his averaging period. The mean of the twelve monthly results are virtually identical with the annual result using ρv and x averaged over the whole year – i.e., the seasonal cycle makes little contribution to the net annual transport.

At 5N: 12 month mean = 1.9, annual mean cell = 1.9×10^{19} cal/day

At 10N: 12 month mean = 1.9, annual mean cell = 1.6×10^{19} cal/day

Now we turn to the Northern Hemisphere transports by the transient eddies (TEs). Here January and July are not the extreme seasons. In fact both represent minima in the sensible heat transport, while April and November are maxima. \therefore we record below the sensible heat transport by transient eddies for all these months.

Latitude	20	30	40	50	60	70
January	0	3	4	4	3	2
April	0	3	5	5	3	2
July	0	0	2	3	2	1
November	0	2	4	4	3	2

January transports are greater than July, but slightly less than April and November. We get a clue to this unexpected behavior by looking at the standing eddy (SE) transport of sensible heat for these same months.

Latitude	20	30	40	50	60	70
January	0	1	4	6	3	0
April	0	0	0	1	1	0
July	0	0	0	0	0	0
November	0	0	1	4	4	1

Here we see that in January, the SE transport exceeds the TE transport, even though in the annual mean it is much less. Also, the SE transport is very sharply peaked in the winter months. This can explain the fall off in the TE transport in January as a negative feed-back: The energy available for driving both kinds of eddies depends basically on the

meridional temperature gradient, as we will see later in the course, and is therefore greatest in January. However, if a greater proportion of the heat is transported by SE's in January than in July, then a smaller proportion needs to be transported by TE's, and the fall off in the January transport can be explained. Note that the total transport, TE + SE, is indeed greatest in January, as we would expect. Furthermore, the seasonal changes in the total eddy flux are much more highly correlated with the seasonal changes in the meridional temperature gradient than are the individual eddy components (see Fig. 3 in Stone & Miller, 1980, *J. Atmos. Sci.*, 37, 1708).

Now let us look at the latent heat transports by the eddies. For the TE's April and November again appear to be greater than January, but the difference is small and may not be significant considering the errors in the data. It is more realistic to say that the seasonal distribution of LH by the TE's is very flat in winter, and we will only present the January and July results. First the TE transports of LH:

Latitude	-10	0	10	20	30	40	50	60	70
January	-1	1	1	2	3	2	1	1	0
July	-1	0	0	0	1	2	2	1	1

Note the shift in the location of the maximum in the transport – this is due to the seasonal shift in the position of the maximum temperature, it being farther north in summer. The LH transport by the SE's is quite different:

Latitude	-10	0	10	20	30	40	50	60	70
January	0	0	0	1	1	1	1	0	0
July	0	0	0	2	2	0	0	0	0

Here the maximum is in summer, and has shifted southward in summer! Actually this low latitude maximum in July is due to a special class of standing eddies, which is strong in moisture content – namely the monsoon circulations, which bring strong rains to India, North Africa, etc. in the summer.

Oort also looked at the contribution to the eddy flux by the seasonal cycle – i.e. the difference between the transport calculated using monthly mean fields and averaging the monthly transports, and the transport calculated using annual mean fields. In this case, significant differences do appear. The maximum total transport by TE's (at 45°N) is 5.8 when calculated from the monthly transports, and 6.8 when calculated from the annual mean fields. This merely demonstrates that there are important transient eddies with time scales longer than a month, but shorter than a year, so that this transport is captured in the second calculation, but not in the first. The maximum total transport by SE's (at 55°N) is 2.3 in the first case, and 1.6 in the second case – i.e., this time a decrease. This merely means that there are SE's on a monthly basis that do not last the year around – i.e. they are TE's, when viewed from the annual mean. Thus the two “seasonal” differences are complementary, and in fact if one adds together both the eddy fluxes, then there is no significant difference between the monthly mean transport and the annual transport.

Now we look at the total meridional flux of SH + LH + PE by all atmospheric dynamical modes. January and July are the extreme months for the total transport, so we give the results for these two months only:

Latitude	-10	0	10	20	30	40	50	60	70
January	0	3	5	6	6	7	10	9	3
July	-6	-2	1	1	2	3	3	3	2

The maxima are actually located at 55° in January and 40° in July. The January maximum transport is > 3 times the July maximum.

Southern Hemisphere: Oort & Peixoto's (1983) analysis of the 10 year data set, May, 1963-April, 1972, included more rawinsonde stations (~1100) than the preceding 5 year period (~900), and they added surface ship data to improve coverage over the oceans. The increased coverage was good enough, that they made global analyses, from 90S to 90N. However, coverage over the Southern Hemisphere oceans was still pretty sparse, so they regard the results for 30S to 70S as "tentative". One difference in their analyses from their earlier ones is that TE statistics for the months and seasons no longer include interannual variations – i.e., SE & TE statistics were calculated for each month of each year, and were then averaged from the 10 individual analyses. Also note that the ship data affected the 1000mb analysis very strongly and the 1000mb analyses do not appear to be compatible with those at higher levels because they imply statically unstable lapse rates.

Figure 39 in Oort & Peixoto (1983) shows how \bar{F}_A is broken down into SE, TE and MMC components for the year and seasons. The Northern Hemisphere results are very similar to those of Oort (1971). In the Southern Hemisphere we note:

- 1) Seasonal changes are much smaller in mid-latitudes than in the Northern Hemisphere.
- 2) SE's are negligible, unlike the Northern Hemisphere.

Both of these results are to be expected because of the much greater ocean area in the Southern Hemisphere, which increases the heat capacity of the surface, thereby damping out seasonal changes, and reduces the zonal asymmetries which force SE's.

Vertical Fluxes:

ref: Hantel, 1976, *JGR*, 81, 1577.

The important vertical fluxes in the atmosphere are radiation and the dynamical fluxes of SH, LH, and PE. The radiative flux is known accurately at the ground and the top of the atmosphere, and values at intermediate levels can be calculated if the vertical structure is given. The dynamical fluxes can be broken up into fluxes by the mean vertical circulations, which can be calculated from observations, and by the eddies, which cannot. Thus the eddy fluxes can only be calculated as a residual, and this is what Hantel has done. He divides the Northern Hemisphere into 16 boxes of equal mass, as follows:

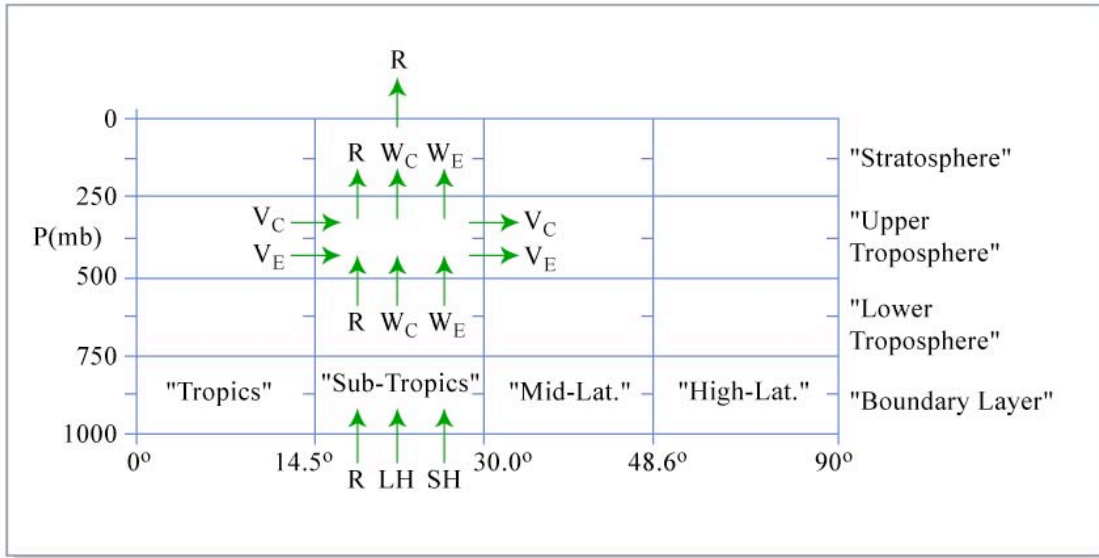


Figure by MIT OCW.

and he considers the balance in each box, as indicated. The definitions are (all quantities are averaged zonally and in time):

- R = net radiative flux (short wave + long wave)
- V_C = meridional flux by MMC (SH + LH + PE)
- V_E = meridional eddy flux (SE + TE)(SH + LH + PE)
- W_C = vertical flux by MMC (SH + LH + PE)
- W_E = vertical eddy flux (SE + TE)(SH + LH + PE)
- LH = surface flux of latent heat
- SH = surface flux of sensible heat

The calculations were done for the extreme seasons (December/January/February and June/July/August), and the storage terms were neglected.

The V_C and W_C fluxes were taken from Oort & Rasmusson's (1971) analyses. An important point concerns how V_C and W_C were calculated. If $h = C_p T + gz + L_v q$, then these transports are proportional to (in pressure coordinates)

$$F_y = [v][h]; \quad F_p = [\omega][h];$$

$$\text{By definition, } \frac{\partial [v]}{\partial y} + \frac{\partial [\omega]}{\partial p} = 0$$

Therefore, if $[h] = \text{constant}$, say h_0 , then

$$\nabla_{2D} \cdot \bar{\vec{F}} = 0, \text{ but } F_y, F_p \neq 0.$$

Thus there is a mean flux carried by the cell which has no physical significance. If we let

$$[h] = h_0 + h''; F_y'' = [v]h''; F_p'' = [\omega]h''$$

And pick $h_0 =$ Northern Hemisphere mean h (Hantel's choice), then

$$\nabla_{2D} \cdot \bar{\vec{F}} \sim \frac{F_p''}{H}, \frac{F_y''}{L} \ll \frac{F_p}{H}, \frac{F_y}{L}$$

$\therefore F_p''$ and F_y'' are the physically meaningful fluxes. If we used F_p rather than F_p' , the role of W_C would appear to be greatly magnified, but in fact most of the divergence associated with it would be cancelled by the divergence associated with V_C and would not affect the temperature structure. \therefore in his analysis, Hantel calculated V_C and W_C from Oort & Rasmusson's data, but with the mean h subtracted from $[h]$.

The surface LH and SH fluxes were taken from Budyko's (1964) estimates. The long and short wave radiation at the top of the atmosphere was taken from Vonder Haar and Suomi's (1971) analysis of satellite data, corrected to be in global balance (an adjustment of a few percent). These provided boundary conditions for the calculation of R at other levels, which was calculated from approximate integrations of the radiative transfer equation. To do the calculation, the following had to be specified from observations in addition:

- 1) Vertical profiles of T , q , CO_2 , O_3 and dust.
- 2) Average $\cos(\text{solar zenith angle})$ for the appropriate season
- 3) Cloud distribution (cloud cover at 14 levels were used)
- 4) Cloud properties (albedo & emissivity) (zero depth assumed)
- 5) Surface albedo and emissivity.

Comparison with independent calculations of radiative fluxes indicated good agreement except in summer higher latitudes.

In calculating W_E as a residual, note that for each vertical column, there are 4 boxes which must be in balance, but only three unknown quantities, W_E at 750, 500, and 250mb. Thus in general there are 4 equations in 3 unknowns. However, these equations are not independent, since each column must individually be in balance, e.g., if we add up the 4 balance equations, the W_E 's drop out, and we end up with a relation between the other fluxes which must be satisfied. Thus in theory there is no indeterminacy. In practice, since the data for R , V , LH, and SH came from different sources, and contain errors, the columns are not quite in balance, and the 4 equations are not quite consistent. Thus Hantel picks a solution for the W_E 's which minimizes the imbalances in each box, in a mean square sense. If we knew where the error was, a different approach might be

appropriate. We are essentially assuming the errors are randomly distributed in the vertical.

The method can be illustrated by a column made of two boxes, with fluxes indicated.

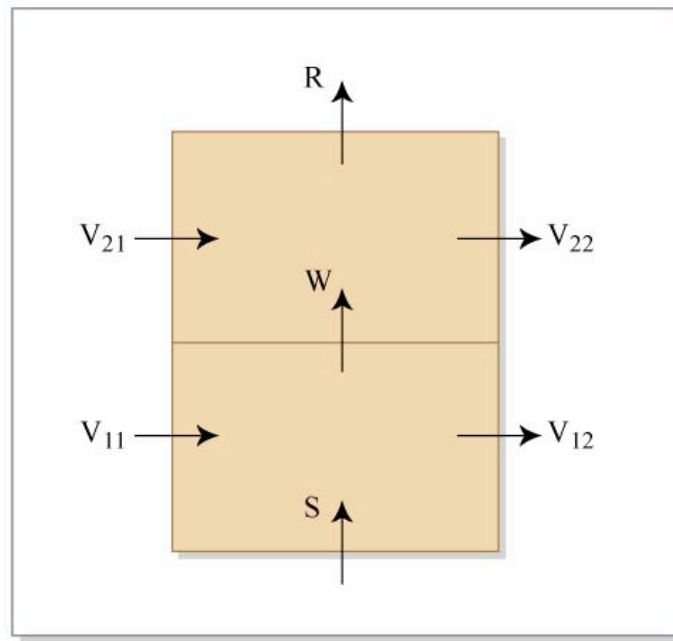


Figure by MIT OCW.

The problem is to determine W when R , S , and all V_{ij} are given, but $V_{21} + V_{11} + S$ does not quite equal $R + V_{12} + V_{22}$. Balances in the two boxes yield the two equations:

$$W = S + V_{11} - V_{12}$$

$$W = R + V_{22} - V_{21} \neq S + V_{11} - V_{12}$$

Define an imbalance for each box, equal to the fluxes in minus the fluxes out:

$$\epsilon_1 = S + V_{11} - W - V_{12} = G_1 - W$$

$$\epsilon_2 = W + V_{21} - R - V_{22} = W - G_2.$$

Now minimize $y = \epsilon_1^2 + \epsilon_2^2$ with respect to W :

$$y = (G_1 - W)^2 + (W - G_2)^2 = G_1^2 - 2G_1W + W^2 + W^2 - 2G_2W + G_2^2$$

$$\therefore \frac{\partial y}{\partial W} = -2(G_1 + G_2) + 4W = 0$$

$$\therefore W = \frac{1}{2}(G_1 + G_2) = \frac{1}{2}[S + V_{11} - V_{12} + R + V_{22} - V_{21}]$$

= “average” solution.

Note that $\epsilon_1 = \frac{1}{2}(G_1 - G_2) = \epsilon_2$. This is always true for any number of boxes. Thus the least squares solution has the same imbalance for each box. Hantel takes this imbalance, which is due to errors in the data, as a measure of the uncertainty in the calculated W’s.

It is always $\frac{1}{N}$ times the imbalance for the total column, where N is the number of boxes – i.e., the imbalance is apportioned equally to all boxes.

Hantel’s results are given in the following table, as the total eddy transport of heat in the vertical, across the surface of each box, in units of 10^{14} Watts. Plus here means upwards:

Latitude		0-14.5°	14.5-30°	30-48.6°	48.6-90°
	250mb	18	8	17	8
June/July/August	500mb	52	34	42	24
	750mb	63	46	49	29
	imbalance	3	5	-7	-4

	250mb	14	-1	16	-1
Dec/Jan/Feb	500mb	39	24	46	21
	750mb	52	39	66	31
	imbalance	2	-1	-6	-2

The transports are generally an order of magnitude larger than the imbalances, and \therefore presumably reliable. They are essentially always upward, as we would expect, and peak near 750mb. There are two latitude peaks in both seasons, one in low latitudes, which it is natural to associate with moist convection, and one in mid-latitudes, which it is natural to associate with large-scale eddies. However, perhaps the subtropical minimum should be associated with an absence of M.C. and large scale eddies. The seasonal change in mid-latitudes is a good deal less than what one would expect from M.C. and the wrong sign. However, the transports in low latitudes peak in summer, and in mid-latitudes in winter, the latter being consistent with TE’s and SE’s.

Hantel also found that, to a first approximation, $\frac{\partial R}{\partial p} + \frac{\partial W_E}{\partial p} \cong 0$, i.e. a sort of radiative-

convection equilibrium obtains in which the radiative flux divergence is approximately balanced by the vertical eddy flux divergence on all scales. For example, in winter,

between 500 and 750mb, and between 30° and 48.6° , the detailed box balance is as follows (the arrows indicate the sign):

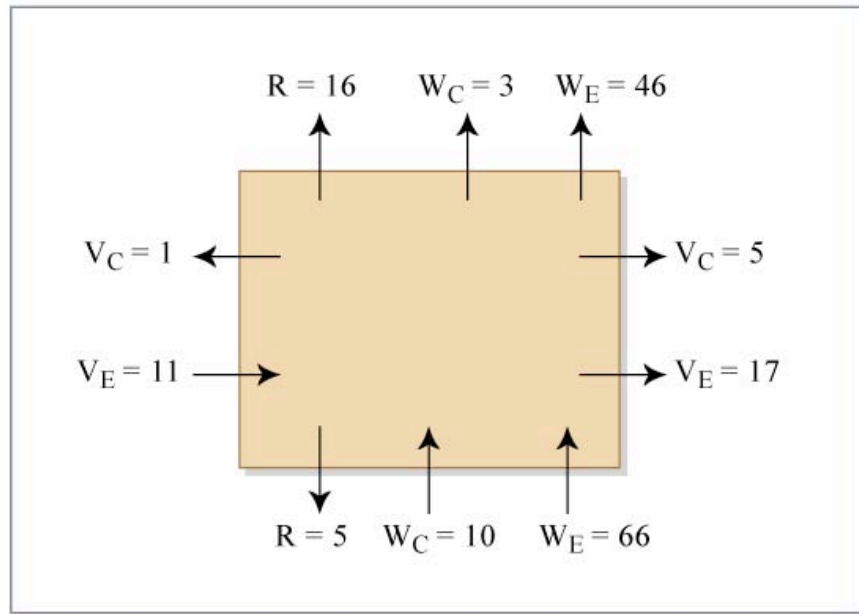
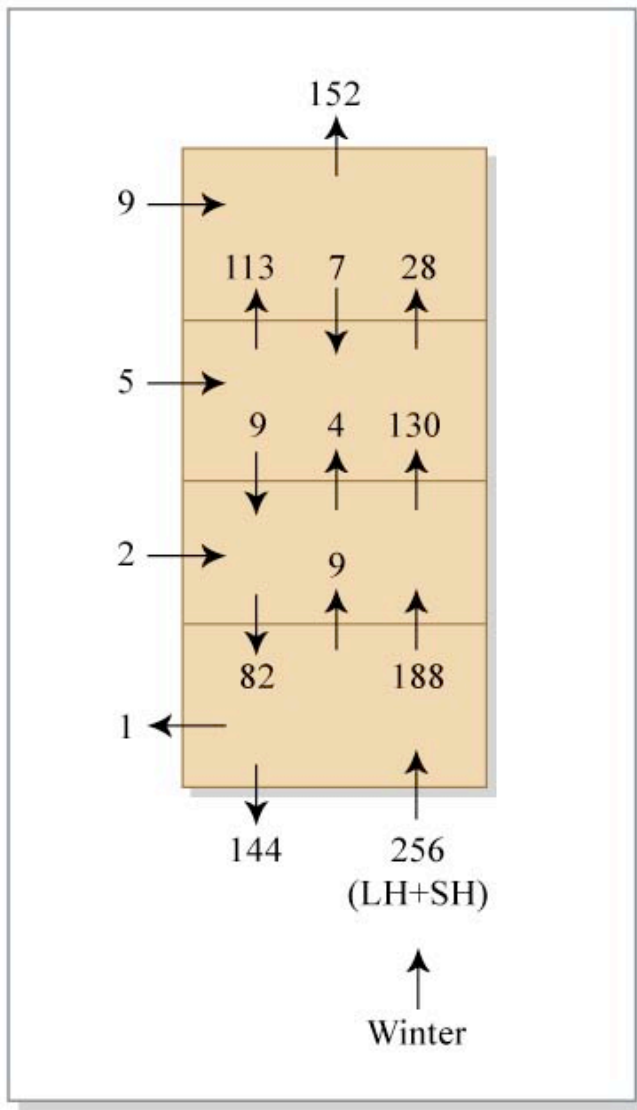


Figure by MIT OCW.

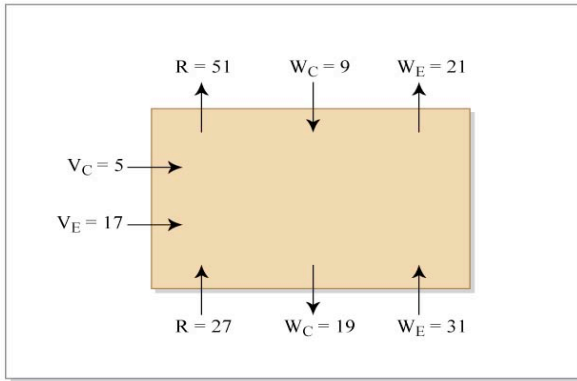
For this box, $\Delta R = +21$; $\Delta W_E = -20$. We also note another typical result, that the vertical dynamical transports are generally an order of magnitude larger than the meridional dynamical transports. Generally R and W_E are the same order of magnitude and the above box is not typical in this respect. The latitudinally integrated fluxes and the resulting balance between R and W_E are illustrated by the following figure for winter and tables for both seasons:



ΔR	ΔW_E	ΔR	ΔW_E
39	-28	47	-51
122	-102	94	-101
73	-58	35	-35
62	-68	54	-39
Jun/Jul/Aug		Dec/Jan/Feb	

Figure by MIT OCW.

The major exception to $\frac{\partial}{\partial p}[W_E + R] \cong 0$ is the polar regions. For example, the detailed box balance between 500 and 750mb and 48.6 and 90° in winter is as follows:



$$\Delta W_E = -10$$

$$\Delta W_C = +10$$

$$\Delta R = +24$$

$$\Delta V_C + \Delta V_E = -22$$

Here, more typically, $|\Delta R| \sim |\Delta V|$, i.e. import of heat from low latitude balances radiative cooling to space.

Hantel's calculation does not enable one to distinguish between SE and TE transports, and between eddy transports of SH and LH. Presumably, in mid-latitudes in winter there is a significant SE contribution. Oort and Rasmusson (1971) actually calculated the vertical transports by SEs, although it is less reliable than the other calculated quantities. According to their results, the stationary eddy heat flux across 500mb in DJF, between 30 and 90N (assuming it is small North of 70° which is certainly a good approximation, because of the small areas), is 4×10^{14} Watts, which may be compared to Hantel's value for the equivalent total eddy transport, of 67×10^{14} W. Apparently the SE's are much less efficient vertical transporters of heat than meridional transporters.

Hantel's calculation of W_E does not distinguish between large scale eddies and small scale convection. Bill Boos in his 2003 term paper for this course calculated the contribution to W_E from large scale eddies from the ECMWF re-analysis. Unfortunately the re-analysis does not include convective and radiative fluxes, so he could only calculate the large scale contribution to W_E . The result for the winter months is shown below, adapted from Figure 13 of his term paper. Hantel's values for W_E are shown for comparison. Since we don't know to what extent the other fluxes that Hantel used, particularly the radiative fluxes, agree with what the ECMWF re-analysis gave, we can only draw qualitative conclusions, based on the assumption that the difference between Hantel's W_E and Boos' calculated large-scale contribution is due to moist convection. The results, however are consistent with what we deduced qualitatively from the seasonal changes in Hantel's results. In particular:

1. convection dominates in the tropics.
2. convection is somewhat larger than the large-scale contribution in the subtropics.
3. the large-scale contribution is somewhat larger than the convective contribution in mid-latitudes.
4. the large scale contribution dominates in high latitudes.

Yang Zhang in her 2004 term paper in this course repeated Boos' calculation, but she used the NCEP re-analysis, and did the calculations for both the winter and summer seasons. Her results for winter were very similar to Boos'. In summer, the conclusions given above still applied, except in high latitudes where she found that the large-scale and convective contributions were comparable in magnitude.

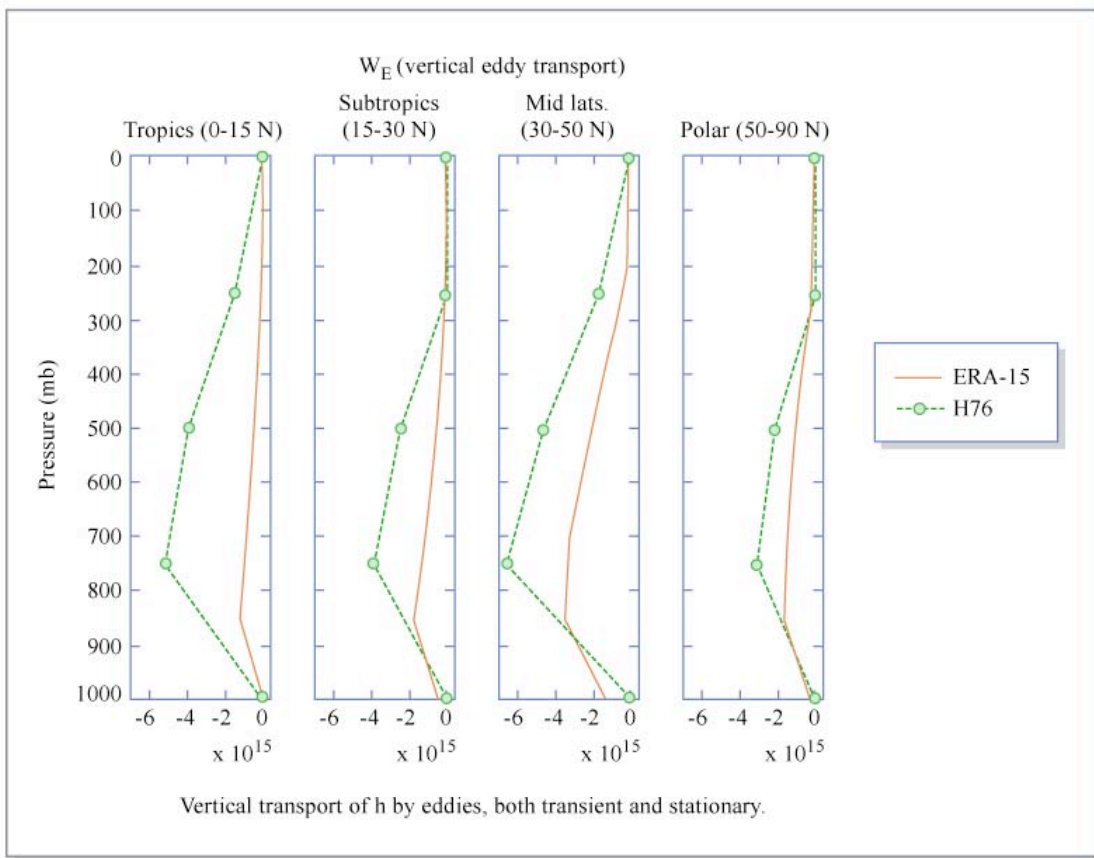


Figure by MIT OCW.

Baroclinic Adjustment: For a long time, the generally accepted theory for why we have TE's in mid-latitudes is that they are due to barocline instability. The Charney-Stern Theorem tells us the conditions under which a zonal mean flow (which is a good description of the time mean state of the atmosphere under most circumstances) can be unstable. For quasi-geostrophic flow on a β -plane, potential velocity is given by

$$q = \frac{\partial v}{\partial x} - \frac{\partial u}{\partial y} + f + \frac{f_0}{\rho_s} \frac{\partial}{\partial z} \left(\frac{\rho_s}{N^2} \frac{\partial \psi}{\partial z} \right),$$

$$\text{where } u = -\frac{\partial \psi}{\partial y}, v = \frac{\partial \psi}{\partial x}, \psi = \frac{P - P_s}{f_0 \rho_0}, N^2 = \frac{g}{\theta_0} \frac{\partial \theta_s}{\partial z},$$

$$\rho_s = \rho_0 e^{-z/H} \quad (\Rightarrow P_s), \theta_s = \theta_s(z); f_0, \rho_0, \theta_0 = \text{constants.}$$

q is a quasi-conserved quantity outside the PBL, because dissipation is small. If $v = 0$, $u = [u]$, then the Charney-Stern Theorem tells us that a necessary condition for $[u]$ to be unstable is that

1. $q_y = \beta - [u]_{yy} - \frac{f_0^2}{\rho_s} \frac{\partial}{\partial z} \left(\frac{\rho_s}{N^2} \frac{\partial [u]}{\partial z} \right) = 0$, or
2. $\frac{\partial \theta}{\partial y} < 0$ at $z = 0$ (in the Northern Hemisphere).

Although these are not sufficient conditions, it generally requires pathological conditions for $[\bar{u}]$ not to be unstable when #1 or #2 are satisfied. In the atmosphere, #2 is generally satisfied, and may be thought of as potentially the main source of baroclinic instability in the atmosphere. (Climatological data do show zeros in q_y near the top of the planetary boundary layer, but the instabilities associated with them are much weaker than those associated with the temperature gradient at the ground. See Fullmer (1982).) As Booker and Bretherton showed, #1 and #2 may be combined by generalizing the definition of q_y to

$$q_y = \beta - [u]_{yy} - \frac{f_0^2}{\rho_s} \frac{\partial}{\partial z} \left(\frac{\rho_s}{N^2} \frac{\partial [u]}{\partial z} \right) - \frac{f_0^2}{N^2} \frac{\partial [u]}{\partial z} \Big|_{z=0} \delta(z)$$

where $\delta(z)$ is a delta function at $z = 0$. (Recall the thermal wind equation,

$$f_0 \frac{\partial u}{\partial z} = - \left(\frac{g}{\theta_0} \right) \frac{\partial \theta}{\partial y}.)$$

Thus baroclinic instability can always be associated with the presence of a zero in q_y , and, since $\beta > 0$, this in turn is associated with flows such that

there is a region where $q_y < 0$. The δ function guarantees this at $z = 0$ if $\frac{\partial [u]}{\partial z} > 0$.

The baroclinic adjustment hypothesis essentially asserts that the eddies that arise because of baroclinic instability will act to stabilize the flow by eliminating regions where $q_y < 0$.

Stone and Nemet (1996) explored the implications of this, and looked at atmospheric observations to see if one can identify the signatures of such behavior. They noted that

$$\frac{[u]_{yy}}{\frac{f_0^2}{\rho_s} \frac{\partial}{\partial z} \left(\frac{\rho_s}{N^2} \frac{\partial [u]}{\partial z} \right)} \sim \frac{N^2 H^2}{f_0^2 L^2} \sim \frac{L_r^2}{L^2},$$

where L_r = radius of deformation, and L = y-scale of $[u]$, and that this ratio = $O(10^{-1})$ when calculated from observations, as one would expect since $L_r \sim 1000\text{km}$, $L \sim 3000\text{km}$. Thus one can approximate

$$q_y \equiv \beta - \frac{f_0^2}{\rho_s} \frac{\partial}{\partial z} \left(\frac{\rho_s}{N^2} \frac{\partial [u]}{\partial z} \right) \text{ for } z > 0.$$

$$\text{Define } h = \frac{f_0^2 \frac{\partial [u]}{\partial z}}{\beta N^2} = \frac{f_0}{\beta} \left(\frac{-\frac{g}{\theta_0} \frac{\partial \theta}{\partial y}}{\frac{g}{\theta_0} \frac{\partial \theta_s}{\partial z}} \right)$$

= $a \tan \phi \left(\frac{\partial z}{\partial y} \right)_\theta$. (Thus h is proportional to the slope of the isentropes. It is also an

important parameter in baroclinic instability theory, namely, the characteristic vertical scale of a baroclinic instability when β is large, or $h \ll H$.) Thus the baroclinic adjustment hypothesis says that the eddies will tend to produce a state such that

$$q_y \geq 0 \text{ for } z > 0, \text{ i.e. } \beta \left\{ 1 - \frac{1}{\rho_s} \frac{\partial}{\partial z} (h \rho_s) \right\} \geq 0.$$

Let us call the state with $q_y = 0$ the adjusted state, $h = h_{\text{adj}}$. We can integrate to find:

$$\frac{\partial}{\partial z} (h_{\text{adj}} \rho_s) = \rho_s = \rho_0 e^{-z/H},$$

$$h_{\text{adj}} \rho_0 e^{-z/H} = -H \rho_0 e^{-z/H} + \text{constant}.$$

Now we can satisfy the second part of the Charney-Stern theorem, i.e., make $q_y = 0$ at $z = 0$ as well, by choosing the constant so $h_{\text{adj}} = 0$ at $z = 0$.

Thus $h_{\text{adj}} \rho_0 e^{-z/H} = H \rho_0 \left(1 - e^{-z/H}\right)$, or

$$h_{\text{adj}} = H \left(e^{z/H} - 1 \right)$$

Note that h is “adjusted” by two effects of baroclinic eddies (as will be discussed later in talking about the energy cycle). These eddies transport heat down the meridional T gradient, and \therefore tend to decrease $\frac{\partial[u]}{\partial z}$, and they transport heat upward, and \therefore tend to increase N^2 . Thus these eddies decrease h below the values they would otherwise have. Suppose $h = h_e$ are the values that h would have in the absence of eddies. Then one would expect

$$h_{\text{adj}} < h < h_e .$$

If the eddies are very efficient at “adjusting”, then h will $\cong h_{\text{adj}}$; if they are inefficient, h will $\cong h_e$. If $h_{\text{adj}} > h_e$ (stable, which one expects high in the atmosphere because N^2 increases and $\frac{\partial[u]}{\partial z} \rightarrow 0$ at the maximum in the jet, and at low latitudes because $\tan \phi \rightarrow 0$.) then there are no eddies or adjustment, and the theory postulates that $h \cong h_e$. This is consistent with our knowledge that instabilities that arise because of #2 in the Charney-Stern Theorem, decay exponentially away from the ground. Fig.1 in Stone and Nemet (1996) illustrates the behavior that one then expects. (Note that in the PBL, where eddies are suppressed by dissipation and the boundary condition $w = 0$ at $z = 0$, one expects the adjustment to be much weaker.)

h calculated from observations is shown for January in Fig. 2 of Stone & Nemet at various latitudes. In fact we see that $h \cong h_{\text{adj}}$ (but $> h_{\text{adj}}$) for $\phi \geq 28^\circ$ and $2\text{km} \leq z \leq 6\text{km}$ (800 to 500mb). Model calculations in these regions indicate that h_e is $\gg h$ -- e.g., at 45° , 4km , $h_e = 30$ to 60km . Thus there does appear to be a region of baroclinic adjustment in the lower troposphere, in mid-latitudes. Higher up, we do get a rather sharp transition to conditions where $h < h_{\text{adj}}$, implying that eddies are not having much effect. Fig. 4 in Stone and Nemet shows the seasonal changes at 46° . The adjusted region is there in all seasons, and the changes in h are relatively small in this region, in spite of the large changes in atmospheric heat transport (> 3 times). This implies that the eddies are in fact very efficient at “adjusting” the structure of the atmosphere, i.e., they respond to changes in the forcing in such a way as to keep h and the isentropic slopes close to their “adjusted” values.